Food Chemistry 450 (2024) 139369

Contents lists available at ScienceDirect

Food Chemistry

journal homepage: www.elsevier.com/locate/foodchem

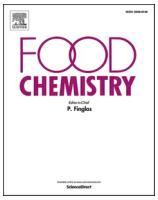

Stabilizing interactions of casein microparticles after a thermal post-treatment

Ronald Gebhardt *, Calvin Hohn, Md Asaduzzaman

RWTH Aachen University, Chair of Soft Matter Process Engineering (AVT.SMP), Germany

ARTICLE INFO

Keywords:
Casein microparticles
Carrier material
Swelling
Thermal post-treatment
Thiol-exchange reaction
System dynamics modelling

ABSTRACT

Casein microparticles from milk are important carrier materials for bioactive substances with stability and swelling properties that can be influenced by heat treatment. Microparticles produced by depletion flocculation and film drying remain stable in acidic media but swell and disintegrate under slightly alkaline conditions. Heat treatment after formation can stabilize the microparticles via a disulfide bridge network and newly formed hydrophobic contacts. Temperatures >60 °C are required so that denatured whey protein initiate formation of disulfide bridges via thiol exchange reactions. The particles then swell in a two-step process and exhibit an overshooting effect. If formation of disulphide bridges is prevented during heat treatment by adding *N*-methylmaleimide, overshooting swelling disappears and microparticles continue to expand instead. The analysis with parallel system dynamics models is based on the swelling of uncross-linked caseins, which is limited by the expansion capacity of cross-linked caseins.

1. Introduction

Casein micelles in milk are natural nanocarriers for calcium phosphate (Dalgleish, 2011). They provide newborns with this poorly soluble mineral in colloidal form for the formation of bones and teeth and at the same time prevent calcification of the breast tissue (Farrell Jr, Malin, Brown, & Qi, 2006; Holt, Carver, Ecroyd, & Thorn, 2013; Antuma, Stadler, Garamus, Boom and Keppler, 2024). Casein micelles are also excellent nano-vehicles for encapsulation and delivery of hydrophobic or poorly soluble nutraceuticals and drugs (Tang, 2021). Several scientific papers exist on the production strategies and applications (Cohen et al., 2017; Menéndez-Aguirre et al., 2014). Casein micelles must be aggregated to produce casein microparticles, which is achieved by loss of colloidal stability using acidification, high-pressure or thermal processes (Mezzenga & Fischer, 2013). For the encapsulation of globular proteins and probiotic cells in microparticles, transglutaminase (TGase) or genipin are used for the covalent cross-linking of the caseins (Heidebach, Först, & Kulozik, 2009a; Song, Zhang, Yang, & Yan, 2009). However, the stability of the microparticle can also be achieved by non-covalent contacts, e.g. after enzymatic treatment of the casein micelles using chymosin (Heidebach, Först, & Kulozik, 2009b). Casein micelles are approx. 100–300 nm large, spherical association colloids consisting of different polypetide chains (α_{S1}-, α_{S2}-, β- and κ-casein) and colloidal calcium phosphate. Cryo-transmission electron tomography and various SAXS techniques revealed a sponge-like organization of the micelles with water-filled domains or channels (Bouchoux, Gésan-Guiziou, Pérez and Cabane, 2010; Trejo, Dokland, Jurat-Fuentes, & Harte, 2011; Takagi, Nakano, Aoki, & Tanimoto, 2024). Inside the micelles, α- and β-caseins interact through their hydrophobic domains or form contacts via the colloidal calcium phosphates using the phosphoseryl clusters in the primary structure (Bijl, Huppertz, van Valenberg, & Holt, 2019). In contrast, the κ-caseins are localised on the surface, whereby the hydrophobic part is anchored in the interior while the hydrophilic part protrudes approx. 7 nm into the environment and contributes to colloidal stability as an extended polymer brush (De Kruif & Zhulina, 1996).

Both α_{S1}- and κ-casein can participate in thiol-disulfide exchange reactions due to their sulfhydryl groups (Lowe et al., 2004). In heated milk, disulphide bridges are formed with whey proteins, which influences, for example, the water-binding behavior and the elastic properties of the gelled products made from it (Vasbinder, Alting, Visschers, & de Kruif, 2003; Mahomud, Haque, Akhter and Asaduzzaman, 2021). The effects caused by disulphide bridges can be prevented by adding thiol-blocking agents such as N-ethylmaleimide, NEM. However, the concentrations used to completely prevent disulphide bridges vary between 0.07 and 20 mM NEM depending on the study and the milk

* Corresponding author.
E-mail address: ronald.gebhardt@avt.rwth-aachen.de (R. Gebhardt).

https://doi.org/10.1016/j.foodchem.2024.139369
Received 9 February 2024; Received in revised form 11 April 2024; Accepted 12 April 2024
Available online 16 April 2024

system investigated (Vasbinder et al., 2003).

While many studies focus on the structure of casein micelles and the binding and encapsulation of bioactive substances, there is a lack of research on the physicochemical properties of casein capsules, their structural composition and the methods for their extraction and characterisation (Acuña-Avila, Cortes-Camargo, & Jiménez-Rosales, 2021). In recent years, our research group has developed a gentle preparation method for a casein micelle-based microparticle system and various methods to analyze and predict its pH-dependent stability and swelling behavior. The casein microparticles (CMPs) are formed by pectin-induced depletion flocculation followed by film drying (Zhuang, Sterr, Kulozik and Gebhardt, 2015). The CMPs, which are then obtained from the pectin matrix by enzymatic hydrolysis, swell in a two-stage process in media with pH > 7.5 until they disintegrate (Schulte, Stöckermann, & Gebhardt, 2020). The higher the pH value of the medium, the faster the swelling and decomposition process takes place. A statistically relevant number of observations showed that the rates of the swelling steps are not dependent on the initial size of the particles and that CMPs retain their spherical shape until disintegration (Schulte, Pütz, & Gebhardt, 2021). The changes in the microscopically observable particle area can then be interpreted as volume changes via the spherical approximation and analysed and predicted via the simulation of volume flows (Schulte, Stöckermann, Thill, & Gebhardt, 2020). For this purpose, we use system dynamics modelling, which has already been successfully used in the past to describe the complex kinetics during the processing of biological systems (Gebhardt, Pechkova, Riekel, & Nicolini, 2010; Eedara, Tucker and Das, 2019).

The swelling properties of CMPs can be adjusted by special pre-treatments and targeted processing (Asaduzzaman, Pütz, & Gebhardt, 2022; Schulte et al., 2021). Swelling-induced decomposition can be prevented by rapid media exchange under acidic conditions or by enzymatic crosslinking (Gebhardt, Khanna, Schulte, & Asaduzzaman, 2022; Gebhardt, Pütz, & Schulte, 2023). Recently, we were able to show that thermal post-treatment also stabilizes CMPs, with two different levels of stability existing in the temperature range between 40 and 90 °C (Asaduzzaman & Gebhardt, 2023). While the stabilizing effect in the temperature range up to 60 °C can be attributed to a hydrophobic collapse of the sponge-like structure, the mechanism for preventing swelling-induced decomposition at temperatures >70 °C is still unknown.

In this study, we want to understand the thermal stabilization of CMPs, which could be significant for their resource-efficient development as a swelling-regulated delivery system. Since pasteurisation is usually carried out anyway, an enzymatic post-treatment step could be saved by appropriate thermal process control. After heat treatment at T = 70 °C, we observed an overshooting effect in the swelling curves, which has also been observed in TGase-stabilized CMPs due to newly introduced isopeptide bonds. Therefore, in this work we use turbidity and swelling experiments in combination with structure-breaking chemicals and system dynamics models to identify heat-induced covalent cross-links and characterise their influence on the stability and water-binding properties of CMPs.

2. Material and methods

2.1. Materials

Casein micelle concentrate powder MC80 and whey protein were kindly provided by Milei GmbH Germany and citrus pectin (highly methylated pectin classic CU 201) was obtained from Herbstreith & Fox (Herbstreith & Fox GmbH & Co. KG, Neuenbürg, Germany). Pectinase from Aspergillus niger, Sodium hydroxide, NaOH (1 M), Potassium hydroxide, hydrochloric acid, HCl (1 M), and NEM were purchased from Merck (Merk, Darmstadt, Germany). Sodium dodecyl sulfate (SDS), calcium chloride, $CaCl_2$, BisTris, and all salts (purity >99% or analytical grade) for simulated milk ultrafiltrate (SMUF) preparation were purchased from VWR, Darmstadt, Germany. Milli-Q water was obtained from our lab.

2.2. Preparation of working solutions

The buffer solution (50 mM BisTris, 10 mM $CaCl_2$) was prepared in milli-Q water, the pH of which was adjusted to 6.8 by adding 1 M HCl and stored at 4 °C for further use. The formulation of SMUF was based on a simple and reliable method described by Dumpler, Kieferle, Wohlschläger, & Kulozik, 2017. The SMUF solution was prepared in milli-Q water by adding all salts in a stepwise fashion and letting it dissolve completely before the next salt was added. The pH of the solution was adjusted to 6.7 with dilute HCl solution and stored at 4 °C for further use. Pectinase enzyme solution (activity ≈ 36 units/mL) was prepared by mixing 4.5 mL pectinase (Pectinase from *Aspergillus niger*, activity ≈ 800 units per mL) with 100 mL BisTris buffer (pH 6.8).

2.3. Preparation of casein microparticle

The depletion flocculation interaction between pectin and casein micelles under neutral pH conditions formed the basis of the CMPs production process (Zhuang, Sterr, Kulozik, & Gebhardt, 2015). CMPs were prepared in accordance with a protocol outlined by Schulte, Stöckermann, Thill, & Gebhardt, 2020. Briefly, a micellar casein solution (7.36%) was prepared by dissolving casein micelle powder (MC80, Milei GmbH, Germany) in SMUF at pH 6.7. The dispersion was agitated (at 150 rpm) for 1 h at room temperature, 4 h at 4 °C, and a further 1 h at 37 °C to ensure that the micellar structure was adequately hydrated. A 2% pectin (CU 201, Herbstreith & Fox GmbH & Co. KG, Neuenburg, Germany) was prepared in BisTris buffer by continuous agitation (at 300 rpm) and heating for 3 h at 80 °C then cooled down to room temperature, the pH value of which readjusted to 6.8 using 1 M NaOH. A casein-pectin mix solution (3% casein and 0.3% pectin) was prepared in BisTris buffer at pH 6.8 to allow the pectin-induced formation of casein aggregates. However, the aggregates formed were deformable and therefore compressed and solidified by subsequent film-drying processes. For film formation, an aliquot of 3.9 g mix solution was transferred to a glass petri dish (70 mm) and let dry under the lab environment (T = 20 °C, RH = 50%) for 16 h. Enzymatic hydrolysis of the film was performed by adding 10 mL enzyme solution to each petri dish. The hydrolysis was performed in a ThermoMixer (Eppendorf AG, Germany) with continuous shaking (rpm 150) for 2 h at T = 47 °C. Upon hydrolysis, the turbid supernatant solution was carefully collected and centrifuged (at RCF 1500, T = 22 °C for 10 min). After centrifugation, the clear supernatant was poured out and the resulting pellet containing CMPs was redispersed in BisTris buffer solution (pH 6.8) and stored at T = 4 °C or used for further post-treatments.

2.4. Post-treatment of CMPs

After preparation, one part of the CMPs sample was used for the addition of whey protein (0.0025%), while the other part was used for the addition of NEM at different concentrations with BisTris buffer. Both samples were post-heated at T = 80 °C for 2 h. After heat treatment, the samples were immediately cooled and stored at 4 °C for further analysis.

2.5. SDS stability experiments

For stability analysis, the turbidity of the CMPs solution was measured using a Lambda 365 UV/VIS spectrometer (PerkinElmer, USA) according to the method, which was already used previously (Asaduzzaman et al., 2022). BisTris buffer was used as blank. Briefly, 1.5 mL CMPs dispersion was placed in a semi-micro cuvette (Eppendorf AG, Germany). The turbidity of the sample was measured at a wavelength of 600 nm, slit width of 1 nm and absorbance was recorded for 900 s. Immediately after measurement, 40 μL SDS solution (520 mM in water)

was added to CMPs dispersion, gently mixed up, and measured again. CMPs samples measured in duplicate.

2.6. Swelling experiments

The swelling behavior of CMPs was monitored by applying exchange media (ultrapure water, pH 11) in a sieve cell according to the protocol developed by Schulte (Schulte, Stöckermann, Thill, & Gebhardt, 2020). Briefly, the swelling chamber was filled with CMPs dispersion (in BisTris buffer, pH 6.8) and placed under Leica DMIL LED inverted microscope (Leica Microsystems, GmbH, Wetzlar, Germany) connected with a Basler camera (Basler AG, Ahrensburg, Germany). The dispersion was allowed to stand for approx. 10 min to sediment the CMPs into the sieve holes. A PHD ULTRA™ syringe pump (Harvard Apparatus, MA, USA) was connected to the swelling chamber by polyethylene tubes (Ø 0.5 mm). The pump flow rate was set at 0.05 mL per min for the exchange medium. The swelling process of the CMPs was started by replacing the buffer solution with an exchange medium. With the activation of the syringe pump, an image of a single microparticle trapped in the sieve holes was recorded for 2 h at the rate of 2 frames per second using the Basler video recording software. Image frames were extracted using PyCharm (version 2021.1.3, JetBrains, Czech) and the area of the CMPs was calculated by a freehand selection of the particle's outer lines using ImageJ software (NIH, USA). All samples were measured in duplicate.

2.7. System dynamics modelling

Models to analyze the complex swelling kinetics were developed and simulated using Stella 1.6 software (iseesystems.com, Lebanon, NH). The system of underlying differential equations was solved using the Euler integration method with a simulation time step of 0.25 s. For comparison with the experimental data, projected particle areas were calculated from the simulated volume profiles using the spherical approximation, which is a good approximation for CMPs for the entire swelling process (Schulte et al., 2021). The models are based on a parallel model approach developed for heat-treated CMPs (Asaduzzaman & Gebhardt, 2023). The swellable caseins are divided into an uncross-linked and a cross-linked fraction, which are modeled by volume I and volume II (see areas highlighted in red and blue in Fig. 1). The level of volume I changes due to two inflows, which depend on the current volume of the reservoir and on rate coefficients (RCI_1 and RCI_2) activated by step functions σ(t) with characteristic times t_1 and t_2, respectively. However, the increase in volume I is limited by the cross-linked casein fraction, which is described by volume II. This is accounted for by a maximum swelling degree V_∞ and second-order swelling kinetics, which was originally used to describe the swelling of gelatin and cellulose in an aqueous medium (Schott, 1992), but has more recently also been used to analyze the swelling kinetics of casein fibers and TGase-treated CMPs (Thill, Schmidt, Jana, Wöll, & Gebhardt, 2022; Gebhardt et al., 2022). Consequently, the rate of change for volume I in the parallel swelling model is:

$$\frac{d\ volume\ I_t}{dt} = \sum_{i=1,2} RCI_i \bullet \sigma^I_{t,i} \bullet (V_\infty - volume\ I_t)^2 \quad (1)$$

Cross-linked caseins are initially in a relaxed state and do not bind water, so that volume II initially has the value 0. Water binding or trapping and thus an increase in volume II only occurs when casein-casein bonds are stretched. The change in the cross-linked casein network is described by the rate of change for volume II, which depends on the current total volume and the rate coefficient $RCII_1$ (expansion) and on the current volume II and the rate coefficient $RCII_2$ (deswelling to the equilibrium value).

$$\frac{d\ volume\ II_t}{dt} = RCII_1 \bullet \sigma^{II}_{t,1} \bullet totale\ volume_t - RCII_2 \bullet \sigma^{II}_{t,2} \bullet volume\ II_t \quad (2)$$

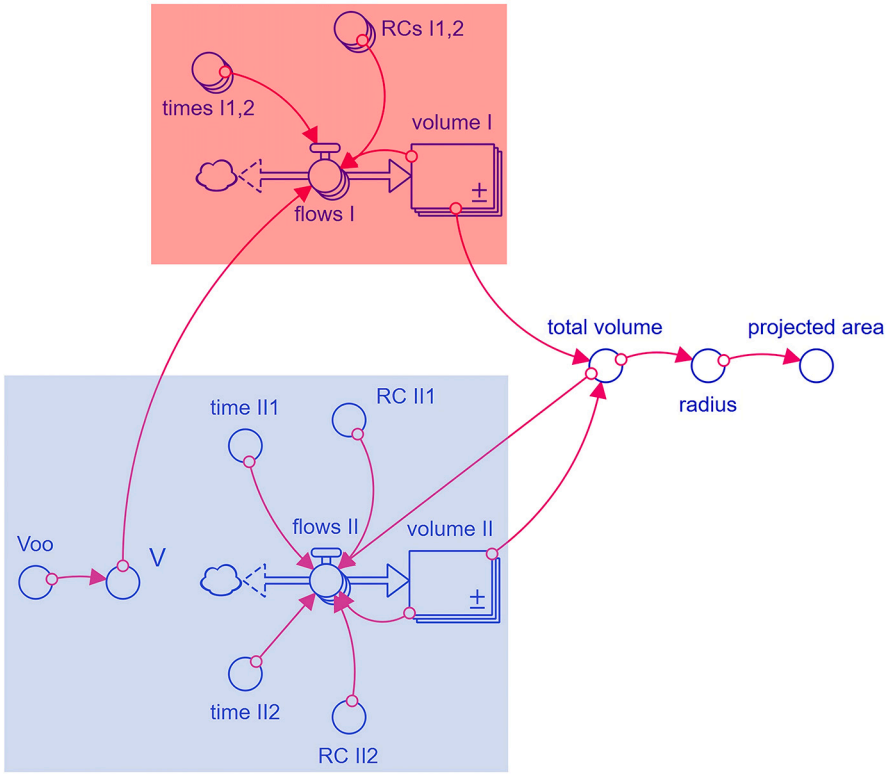

Fig. 1. Parallel dynamic Stella model, which was used to simulate the swelling curves of heat-treated CMPs (Asaduzzaman & Gebhardt, 2023). The microscopically observed particle area is calculated using the spherical approximation from the total volume change resulting from the swelling of uncross-linked (volume I) and cross-linked casein (volume II).

The total volume of CMPs is then obtained by adding the contributions of volume I and volume II.

3. Results and discussions

The nature of interactions stabilizing CMPs after heat treatment at temperatures >60 °C is still unknown. However, the effects are visible in swelling experiments carried out at pH 11 and 20 °C. The typical two-step expansion of untreated CMPs shown in Fig. 2 is then followed by an overshooting effect in case of a heat treatment at 80 °C for 120 min. The corresponding swelling curve shows a maximum after 14 min, followed by a gradual decrease until the swelling equilibrium is reached (Asaduzzaman & Gebhardt, 2023). A similar overshooting effect was also observed in TGase-treated CMPs and was attributed to the collective elastic forces of the newly formed network of isopeptide bonds (Gebhardt et al., 2022). However, since CMPs are made from casein powder with a casein to whey protein ratio of 92: 8%, a disulfide bridge network initiated by denatured whey protein could be responsible for preventing the swelling-induced disintegration of CMPs. To test this hypothesis, we first performed swelling experiments with CMPs to which whey protein was added at different concentrations during the preceding heat treatment. The swelling experiments were performed in microfluidic sieve cells at $T = 20$ °C and the size changes of individual CMPs were observed microscopically as described in previous studies (Schulte, Stöckermann, Thill, & Gebhardt, 2020; Schulte et al., 2021).

Fig. 2 shows that heat-treated CMPs with added whey protein swell more slowly and to a lower final value than was observed in earlier measurements without any addition. For comparison, CMPs with a two-hour heat treatment at 80 °C but without whey protein swell strongly after approx. 8 min. After overshooting, the mean normalized particle area reaches a stable final value after 20 min, which corresponds to four times its initial value (red line, Fig. 2). After the addition of 0.0025% whey proteins, swelling slows down significantly and the final swelling value drops to 1.5 times the initial value. A weak overshooting effect is also observed, which is shifted to longer times. After adding 0.5% whey protein, this effect disappears completely and the swelling is further delayed. The results show that rapid swelling is necessary for the overshooting effect, as already observed in earlier studies with TGase-treated CMPs (Gebhardt et al., 2022). Furthermore, it follows that a maximum stabilizing effect is already achieved at 0.025% WP, since the final swelling value does not decrease further despite a 20-fold increase in the amount of protein to 0.5%. CMPs that were only heat-treated at 60 °C lack these structure-preserving interactions, as shown by the black dashed line in Fig. 2. As with untreated CMPs (red dotted line), the particle area initially increases in two steps up to four times the initial value. However, the CMPs then swell further and much more slowly. After reaching 10 times their original particle area, they were no longer detectable under the microscope. Effective stabilization by heat treatment against swelling-induced decomposition therefore requires both whey proteins and temperatures >60 °C. The results of the experiments suggest that a covalent network of disulfide bonds is formed, which is triggered by heat-denatured whey protein (Lucey, 2020; Mahomud, Haque, Akhter, & Asaduzzaman, 2021).

This requires temperatures >70 °C so that reactive thiol groups of β-lactoglobulin can be exposed after thermal unfolding and thiol-exchange reactions be initiated (Nguyen, Streicher, & Anema, 2018). The reason why CMPs heat-treated at 60 °C swell more slowly and reach higher swelling levels compared to untreated particles has been explained by an internal irreversible restructuring towards a more homogeneous structure (Asaduzzaman & Gebhardt, 2023). A hydrophobic collapse of the sponge-like structure of the CMPs could trigger this structural change, as a maximum hydrophobic effect is observed for proteins between 40 and 80 °C (Van Dijk, Hoogeveen, & Abeln, 2015).

We performed SDS turbidity studies at 20 °C in the presence of different NEM concentrations to understand the influence of disulfide bonds and hydrophobic interactions on the stabilization of CMPs. While SDS weakens hydrophobic contacts between caseins and causes the disintegration of casein micelles and CMPs (Liu & Guo, 2007; Schulte, Pütz, & Gebhardt, 2022), NEM blocks the reactive thiol group, thus preventing the formation of the disulfide bridge network in casein gels (Steinhauer, Kulozik, & Gebhardt, 2014; Vasbinder, van de Velde, & de Kruif, 2004). The decay rates describing the exponentially decreasing SDS turbidity measurements are shown in Fig. 3. The rates influenced by the NEM effect are shown as colored circles (color code will be used further in the following) and compared with reference measurements without NEM from a previous study (Asaduzzaman and Gebhardt, 2023). The rates of the reference measurements showed that with increasing post-treatment temperature, the stability of CMPs towards

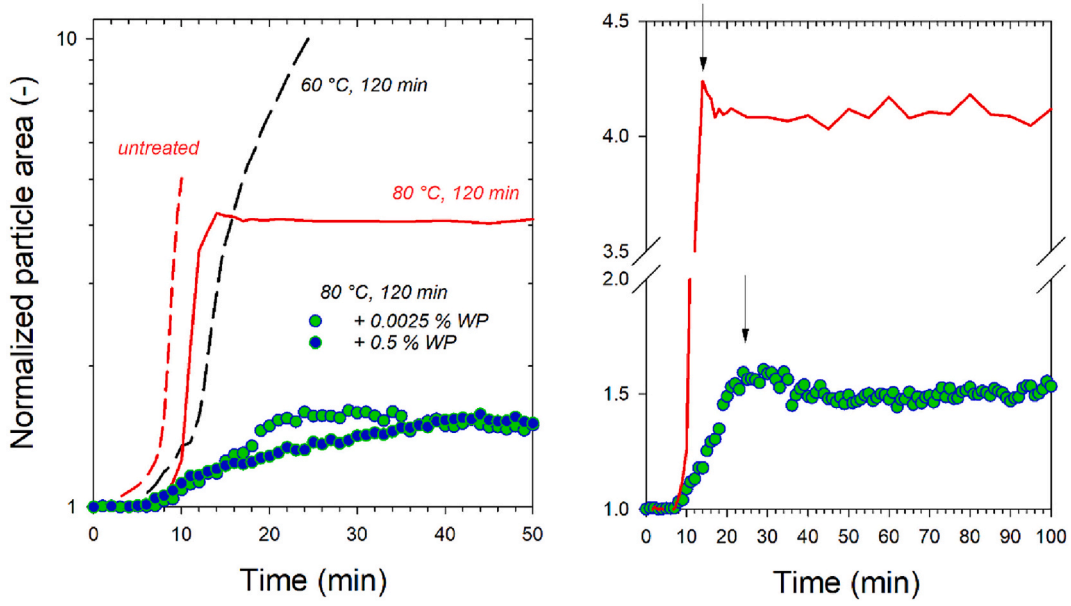

Fig. 2. Influence of added whey protein on the swelling curves of heat-treated CMPs at T = 20 °C. Lines correspond to earlier measurements (Asaduzzaman & Gebhardt, 2023). The post-treatment conditions are shown next to the corresponding swelling data. To emphasize the onset of deswelling (marked by arrows), the relevant data are plotted again on the right side with a linear, broken y-axis.

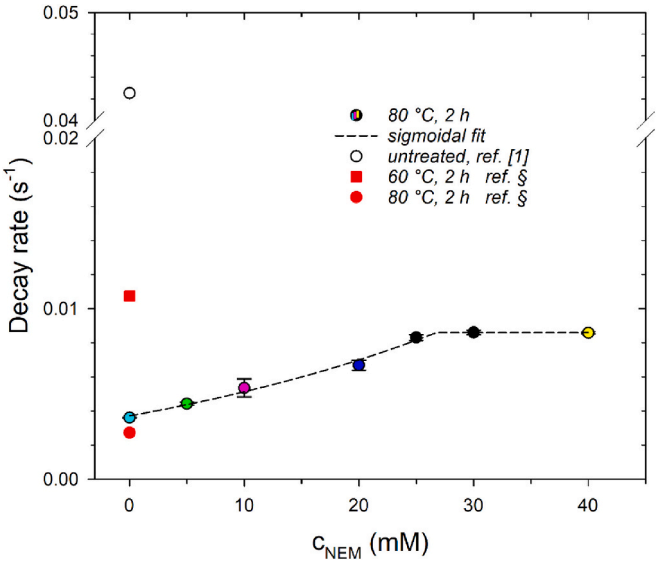

Fig. 3. SDS-decay rates of CMPs heat-treated with different NEM concentrations compared with reference data (ref. §: Asaduzzaman & Gebhardt, 2023).

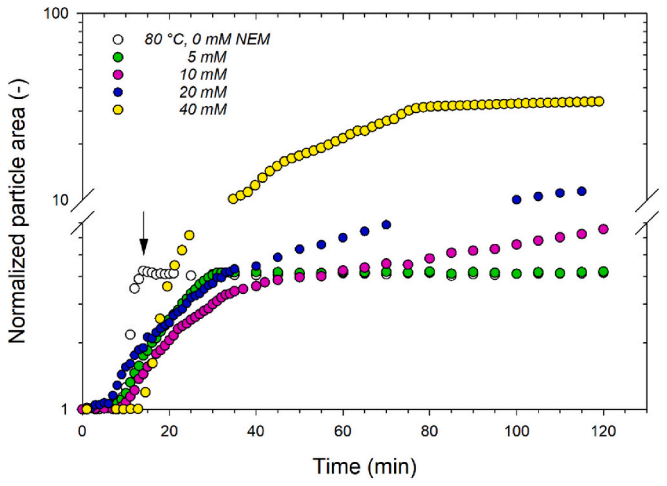

Fig. 4. Normalized particle area of the CMPs as a function of the swelling time at $T = 20$ °C after a jump to pH 11 by rapid buffer exchange. Circles: Measured data of particles heat-treated for 2 h at $T = 80$ °C without and at different concentrations of NEM.

SDS is increased, whereby two different stability levels exist. When post-treatment temperatures between 50 and 60 °C were used, the decomposition rate decreased by about a quarter to 0.01 s^{-1} compared to untreated CMPs. As described above, a hydrophobic collapse of the original porous structure is the reason for the irreversible restructuring and stabilization of the CMPs in this temperature range.

Post-treatment temperatures between 70 and 90 °C once again led to significantly lower rates of approx. 0.002 s^{-1} (Asaduzzaman & Gebhardt, 2023). However, this lowest turbidity reduction rate is not a consequence of decay but rather results from the natural sedimentation of CMPs, which are several μm in size (Gebhardt et al., 2022). The turbidity decreases linearly during sedimentation and exponentially during the decomposition of the CMPs. While the latter dissolve sooner or later, CMPs that settle out can also be observed microscopically after a long time. The rate range between the two stability levels extends over almost one order of magnitude. Based on the rates in this range, the treatment time could be set at 120 min, after which CMPs with 80 °C treatment became completely resistant to SDS. In this study, the sulfhydryl blocker NEM was added to these resistant CMPs (Asaduzzaman & Gebhardt, 2023). As shown in the semi-logarithmic plot of Fig. 3, CMPs become more than proportionally destabilized with increasing NEM concentration until rates remain stable with 0.008 s^{-1} at NEM concentrations >25 mM. The increasing effect of NEM on the SDS stability of the CMPs is best described by a sigmoidal curve with five parameters (see dashed line in Fig. 3). Comparison with the reference measurement of CMPs heat-treated at 60 °C shows that a similar SDS decay occurs for CMPs heat-treated at 80 °C when NEM concentrations above 25 mM are added. Since all thiol groups are blocked by NEM, SDS stability can only be a result of hydrophobic collapse, which is stronger at 80 °C and leads to slightly lower rates than in the reference measurement at 60 °C.

How does the disulfide bridge network influence the swelling properties of CMPs? To answer this question, we conducted further swelling experiments at pH 11 and 20 °C with CMPs to which different amounts of NEM were added during the 80 °C heat treatment. Fig. 4 shows corresponding swelling curves, which are an average of two independently performed single particle swellings. Without NEM (white circles), the swelling data almost correspond to those of previous measurements (compare red line in Fig. 2). As already mentioned, these swelling curves show an overshooting effect after approx. 14 min, which was also observed during the swelling of TGase-stabilized CMPs (Gebhardt et al., 2022). It can be clearly seen that the overshooting effect disappears with NEM and that the CMPs swell more strongly but also more slowly. The overshooting effect during swelling was observed in several polyelectrolyte systems and explained by chain relaxation (Ogieglo et al., 2013; Shieh & Peppas, 1991), ionic interchange and cross-linking (Valencia & Piérola, 2002; Huaman, Vega-Chacón, Quispe and Negrón, 2023) or the formation of hydrogen bonds (Díez-Peña, Quijada-Garrido, & Barrales-Rienda, 2003; Yin, Ji, Dong, Ying, & Zheng, 2008). Both the data shown here and previous results with TGase (Gebhardt et al., 2022) also suggest that the overshooting effect during the swelling of CMPs is related to the covalent cross-linking of casein. Thus, the relaxation of the cross-linked casein chains after their swelling-induced elongation is a plausible explanation for the overshooting effect observed here. However, it is also obvious that the stabilizing effect of heat treatment cannot be completely eliminated by adding 40 mM NEM. The corresponding swelling curve shows that the particle area expands steeply up to 10 times its initial value and then less strongly and only slightly after about 80 min. However, at lower NEM concentrations, the initial swelling is observed to increase much slower compared to the sample without NEM. At 5 mM NEM, the normalized particle area reaches its final swelling value after 30 min, which corresponds to that of the sample without NEM. In contrast, for CMPs with a higher NEM concentration, there is no stable plateau but instead a further expansion, which is stronger at 20 mM than at 10 mM NEM.

For a precise description and detailed analysis of the swelling data, simulations were carried out with a system dynamics model (see Fig. 1), which was extended by processes that occur due to the destabilization of the disulfide bridge network by NEM.

Fig. 5 shows examples of selected simulations of single swelling curves of CMPs to which no (a), 5 mM (b) or 20 mM NEM (c) was added during heat treatment. The simulated solid lines in the swelling curves are calculated using the spherical approximation from the corresponding simulated total volume (black line in Fig. 5, center). Without NEM the swelling is described by the change of two volumes, which refer to the uncross-linked (Volume I) and cross-linked (Volume II) casein fraction. The corresponding simulated volume curve of the cross-linked casein fraction (blue curve, Fig. 5 a2) rises sharply with a slight delay to the uncross-linked portion after approx. 500 s, shows an overshooting effect after approx. 800 s and then stabilizes at a stable swelling value. However, when 5 mM NEM is added during the heat treatment, a part of the previously linked caseins is not cross-linked, because the thiol groups required for this are blocked. As a result, further effects occur during longer swelling times, which make it necessary to extend the current swelling model.

The fraction of uncross-linked caseins increases with increasing NEM

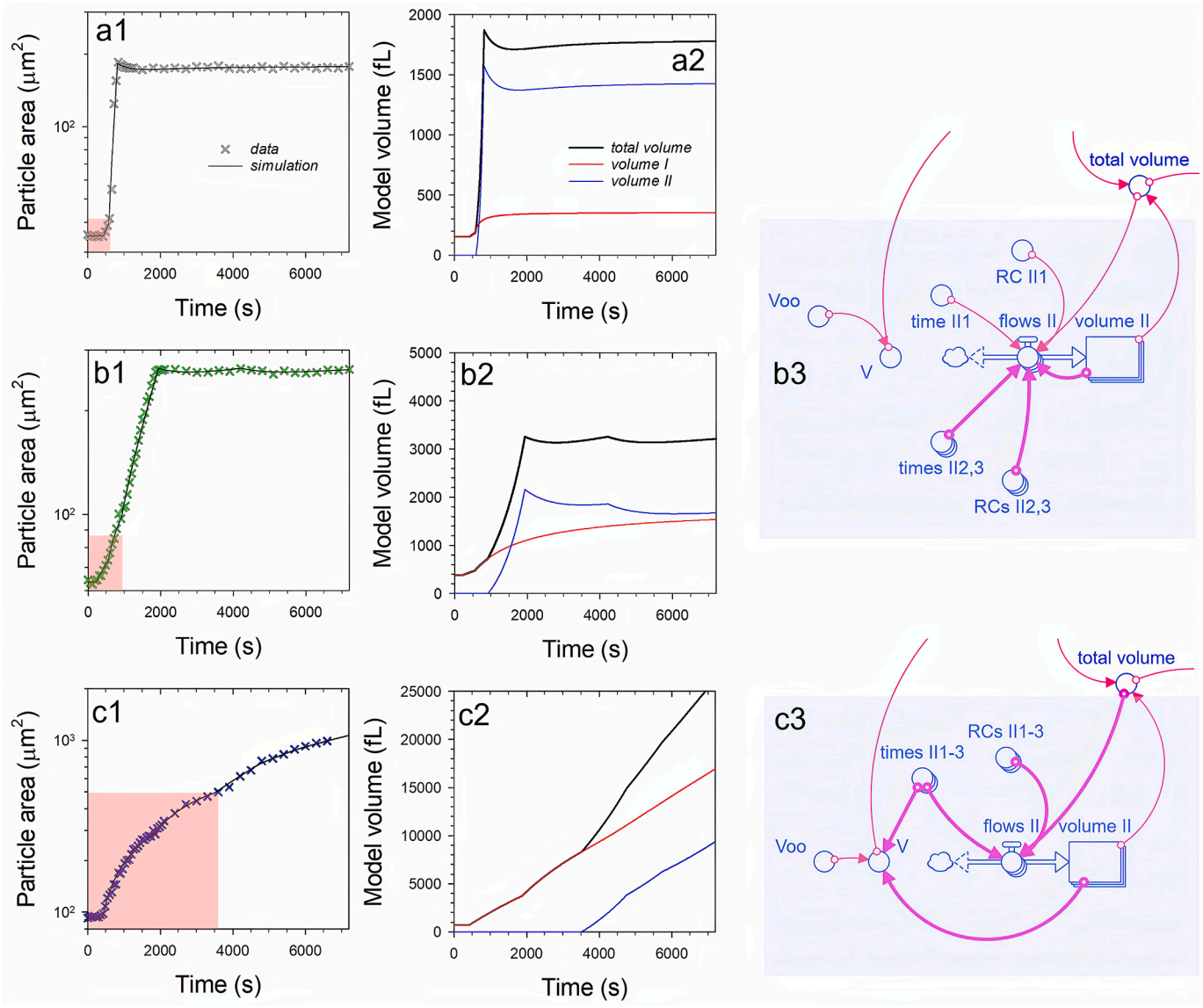

Fig. 5. Swelling curves and simulation with the parallel dynamic model (Fig. 1) of CMPs at pH 11 and T = 20 °C without (a) or with 5 mM (b) or 20 mM NEM (c). Measured data and calculated swelling curves from the simulation results are shown on the left (index 1), the simulated volume flows I and II as well as the total volume flow in the middle (index 2) and required model extensions due to the NEM effect on the right (index 3).

concentration and the effects can be observed both in the swelling data and in the simulation results, i.e. the changes over time of volumes I and II. NEM causes the expansion of the cross-linked caseins (simulated via volume II) to start later and to occur more slowly, resulting in a creeping volume change over time. As a result, the uncross-linked caseins can expand more and more via the typical two-step expansion mechanism (compare red-marked areas in the swelling curves in Fig. 5 a1-c1), as there is less and less resistance to their expansion (see gradual increases in volume I in b2 and c2 instead of the stable final value in a2). To account for the influence of a destabilized disulfide bridge network, the system dynamics model must be modified in the domain of the cross-linked caseins described by volume II (blue marked area in Fig. 1). Fig. 5 (right) illustrates the influencing variables and their dependencies, which determine the structural changes and could play an important role in the modelling of e.g. release kinetics in future encapsulation studies. With an intact disulphide network, i.e. without NEM, swelling and deswelling to a constant swelling value are described for the cross-linked casein component by two volume flows according to eq.2. These depend on a swelling rate coefficient and the instantaneous total volume of the particles and, on the other hand, on a deswelling rate coefficient and the instantaneous value of volume II (Asaduzzaman & Gebhardt, 2023). In contrast, in the presence of NEM, the new two-step effects that appear at the end of the swelling kinetics must be taken into account. The two-step process could occur due to different types of disulphide bridges that can be formed by κ-casein on the one hand and α_{S2}-casein on the other (Lowe et al., 2004). It is plausible that NEM influences the disulphide bridge formation of both caseins differently, as α_{S2}-casein is buried deeper in the micellar structure. This could split the bond strength of the disulphide bridge network and influence the swelling. As a result at least three volume flows must be simulated for the expansion and shrinkage of the cross-linked casein component.

At 5 mM NEM, the disulphide network is still strong enough so that only two step deswelling occurs (Fig. 5 b1). In the dynamic model, this is taken into account by a further volume flow, which depends on the deswelling rate and the instantaneous value of volume II (see Fig. 5 b3). However, at higher NEM concentrations the network becomes unstable and two-step swelling occurs instead of deswelling (see example for 20 mM NEM in Fig. 5 c1). The corresponding graphical model representation in Fig. 5 c3 shows how the origin and consequences of this two-step creeping expansion are taken into account. The volume flows are now all

dependent on the current value of the total volume, as the expansion is caused by the swelling of the uncross-linked caseins. The creeping expansion of the cross-linked caseins also influences the final swelling value, V_∞, which is taken into account in the model via

$$V_\infty^* = V_\infty + \sigma\left(timeII^1\right) \bullet volumeII_t \quad (3)$$

Fig. 6 shows values for the most important model parameters that led to the best simulation result. For the uncross-linked casein fraction (Fig. 6a), the rate coefficients and characteristic times of heat-treated CMPs without NEM are in good agreement with the values reported for the simulation of comparable CMPs preparations in a previous study (Asaduzzaman & Gebhardt, 2023). In general, both steps of the swelling process of the uncross-linked caseins slow down more and more with increasing NEM concentration. This trend can also be observed for CMPs without NEM when the heat treatment was carried out at 60 °C instead of 80 °C. Based on SDS experiments, it was found that new hydrophobic contacts are formed within the CMPs after 60 °C treatment (Asaduzzaman & Gebhardt, 2023). This structural change leads to a more homogeneous internal structure, which persists even after cooling to 20 °C and swells more slowly. Recent in-situ SAXS studies demonstrated similar temperature effects on the internal structure of casein micelles. The micelles are the building blocks for the CMPs and, like them, are sponge-like with water channels and domains throughout the structure (Bouchoux, Gésan-Guiziou, Pérez, & Cabane, 2010; Trejo et al., 2011). After an increase in temperature, water is released from the micelles as a result of hydrophobization (Takagi, Nakano, Aoki, & Tanimoto, 2022). Furthermore, the weight fraction of the protein within the micelles increases during the heating process. In contrast, the number of water domains decreased, but did not change after cooling (Takagi, Nakano, Aoki, & Tanimoto, 2023).

Furthermore, the disulfide bridges formed after treatment at 80 °C mainly link the κ-caseins, which are found at protein-water interfaces due to their amphiphilic character (De Kruif, 1999; De Kruif & Zhulina, 1996). As a result, the originally granular internal structure of the CMPs (Schulte, Stöckermann, Thill, & Gebhardt, 2020) could be partially preserved by the newly formed disulfide bridges during 80 °C treatment. This could also preserve more of the originally existing water channels within the structure during the heat-induced hydrophobic collapse, again resulting in higher swelling rates. Previous studies on casein deposits showed a similar effect. The addition of whey protein and association to casein changed the structure to a porous mass fractal. As a result, a lower specific surface resistance and greater permeate flow were observed (Steinhauer et al., 2014).

The original sponge-like structure of the CMPs disappears due to the NEM influence in favor of a more homogeneous structure, which slows down the swelling processes. As a consequenve, the rates of both swelling steps decrease by almost three orders of magnitude when the NEM concentration is raised from 10 to 40 mM (Fig. 6a). In parallel, the corresponding characteristic times at which the swelling steps occur are delayed by about 1 order of magnitude. A similar observation was also made on membrane deposits in the earlier study. The addition of NEM increased the specific surface resistance and the permeate flux decreased (Steinhauer et al., 2014).

Less precise statements can be made about the swelling/deswelling rates of the cross-linked casein component under the influence of NEM. The values of two (RCII1 and RC II2) of the three rates used for the simulation are in the range between 10^{-3} and 10^{-4} s^{-1} (Fig. 6b). However, a delay in the corresponding characteristic times can also be

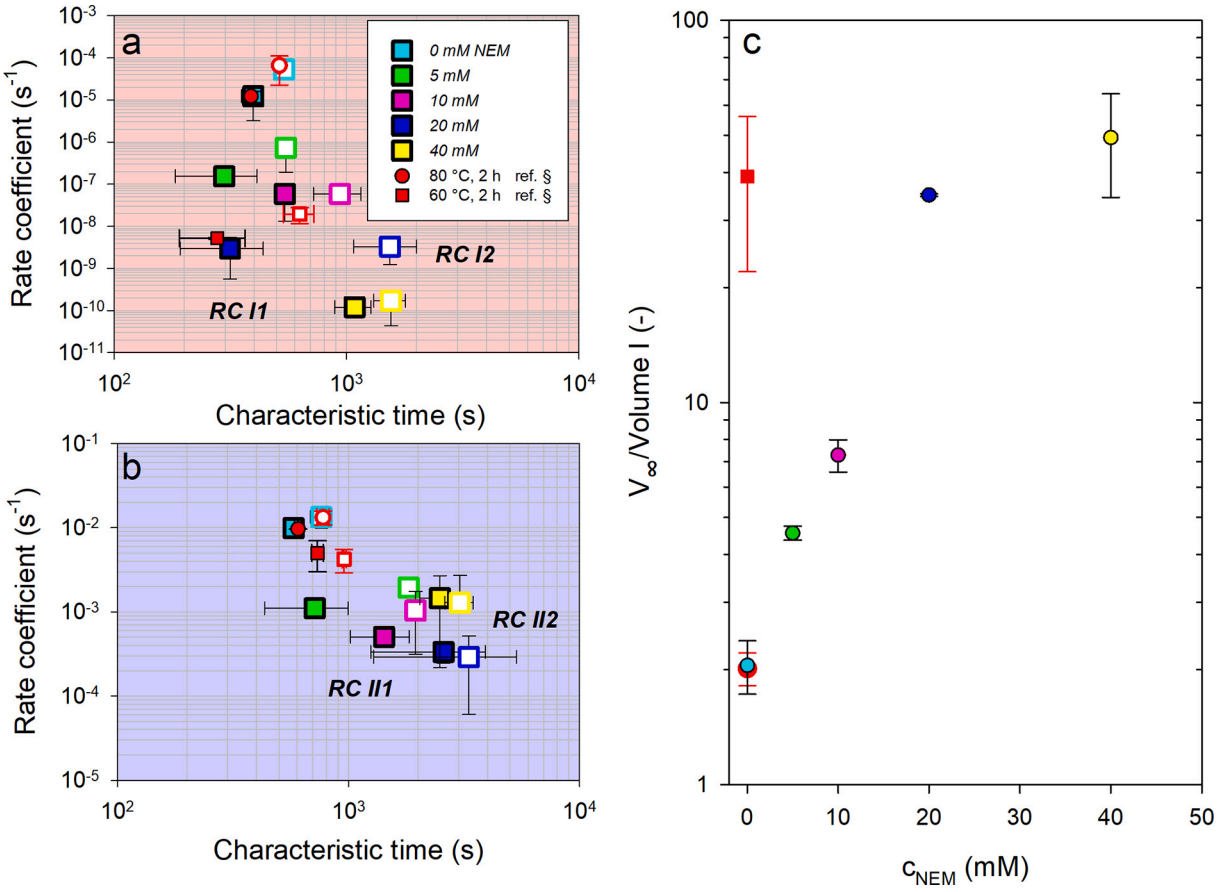

Fig. 6. NEM effect on the most important simulation parameters of swelling curves measured on heat-treated CMPs at 20 °C. a) Rates and characteristic times for the uncross-linked casein fraction; b) Rates and characteristic times for the cross-linked casein fraction resulting from heat treatment; c) Maximum degree of swelling. Reference values for CMPs without NEM after treatment with $T = 60$ °C and 80 °C (ref. §: Asaduzzaman & Gebhardt, 2023).

observed here. The cross-linked casein portion generally swells somewhat later after the characteristic two-step expansion of the uncross-linked caseins (Asaduzzaman & Gebhardt, 2023; Gebhardt et al., 2022). In the dynamic swelling model, this is taken into account by the dependence of the swelling rate of the cross-linked portion on the total volume, which increases due to the swelling of the uncross-linked caseins.

The ratio of the maximum degree of swelling V_∞ to the original volume of the CMPs (Volume I) can be regarded as a measure of the maximum degree of swelling. The results in Fig. 6c show that after a two-hour treatment at 80 °C, the CMPs swell to a maximum of only 2 times their initial volume as also confirming by earlier measurements (Asaduzzaman & Gebhardt, 2023). This earlier study had also shown that CMPs can swell to 30–50 times their initial volume after a comparably long heat treatment at only 60 °C. The results were explained on the basis of irreversible structural changes due to the hydrophobic effect, but could not provide an explanation for the drastic increase in stability after treatment at temperatures >70 °C. The results of this study with NEM show that, in addition to hydrophobic contacts, disulfide bridges in particular prevent stronger swelling. As the NEM concentration increases, the covalent cross-linking decreases and consequently the degree of swelling increases. As with the SDS decay rates (Fig. 3), a plateau value is also reached for the maximum degree of swelling at NEM concentrations between 20 and 40 mM. These plateau values indicate that the structure of the CMPs under these conditions is no longer stabilized by disulfide bridges but rather by hydrophobic contacts similar to CMPs that have been heat-treated at 60 °C.

Our results are consistent with studies on the swelling behavior of internally cross-linked casein micelles. These showed that micelles stabilized by TGase resist swelling-induced disintegration, also when destabilizing agents such as citrate or urea are added to the medium (Huppertz, Smiddy and de Kruif, 2007). In contrast, casein-based gel systems, which are only stabilized by physical contacts, should disintegrate due to swelling (de Kruif, Anema, Zhu, Havea and Coker, 2015). However, neither measurement data nor simulations of this study indicate a complete disintegration of temperature-stabilized CMPs. Rather, stabilities and degree of swelling approach a certain value the more covalent contacts are blocked by NEM.

4. Conclusion

Comparative stability and swelling tests with the thiol group blocker NEM show that a two-hour heat treatment at 80 °C creates a disulphide bridge network that stabilizes the structure of CMPs. The trigger for the formation of disulphide bridges are thiol exchange reactions, which are initiated by denatured whey protein during heat treatment at temperatures >60 °C. The newly inserted chemical cross-links cause the CMPs to no longer disintegrate after the addition of SDS and to expand to a stable final size during swelling. Rapid swelling then leads to overshooting, which is due to the increased elasticity of the newly formed disulphide bridge network. If the thiol groups are completely blocked by NEM, the CMPs become sensitive to SDS and swell up to 30 times their original particle area and remain stable. The decomposition after addition of SDS is similar to CMPs that have only been heat-treated at T = 60 °C and are not stabilized by a disulfide network. However, these disintegrate during swelling when the particle area reaches ten times the original value. This could be due to a weaker hydrophobic collapse of the sponge-like CMPs structure, which is stronger at 80 °C with blocked thiol groups. In the future, corresponding measurements could be repeated with food-grade thiol group blockers such as free cysteine (Lavoisier, Vilgis, & Aguilera, 2019). This could open up new application possibilities for CMPs with regard to the swelling-controlled release of bioactive substances.

CRediT authorship contribution statement

Ronald Gebhardt: Writing – review & editing, Writing – original draft, Visualization, Validation, Supervision, Resources, Project administration, Investigation, Formal analysis, Conceptualization. **Calvin Hohn:** Methodology, Investigation, Data curation. **Md Asaduzzaman:** Supervision, Investigation, Data curation, Conceptualization.

Declaration of competing interest

The authors declare that they have no known competing financial interests or personal relationships that could have appeared to influence the work reported in this paper.

Data availability

Data will be made available on request.

References

Acuña-Avila, P. E., Cortes-Camargo, S., & Jiménez-Rosales, A. (2021). Properties of micro and nano casein capsules used to protect the active components: A review. *Int. J. Food Prop., 24*(1), 1132–1147. https://doi.org/10.1080/10942912.2021.1953069

Antuma, L. J., Stadler, M., Garamus, V. M., Boom, R. M., & Keppler, J. K. (2024). Casein micelle formation as a calcium phosphate phase separation process: Preparation of artificial casein micelles through vacuum evaporation and membrane processes. *Innovative Food Sci. Emerg. Technol., 103582*. https://doi.org/10.1016/j.ifset.2024.103582

Asaduzzaman, M., & Gebhardt, R. (2023). Influence of post-treatment temperature on the stability and swelling behavior of casein microparticles. *Macromol. Mater. Eng., 308*(4), 2200661. https://doi.org/10.1002/mame.202200661

Asaduzzaman, M., Pütz, T., & Gebhardt, R. (2022). Citrate effect on the swelling behaviour and stability of casein microparticles. *Sci. Rep., 12*(1), 18401. https://doi.org/10.1038/s41598-022-23096-x

Bijl, E., Huppertz, T., van Valenberg, H., & Holt, C. (2019). A quantitative model of the bovine casein micelle: Ion equilibria and calcium phosphate sequestration by individual caseins in bovine milk. *Eur. Biophys. J., 48*, 45–59. https://doi.org/10.1007/s00249-018-1330-2

Bouchoux, A., Gésan-Guiziou, G., Pérez, J., & Cabane, B. (2010). How to squeeze a sponge: Casein micelles under osmotic stress, a SAXS study. *Biophys. J., 99*(11), 3754–3762. https://doi.org/10.1016/j.bpj.2010.10.019

Cohen, Y., Levi, M., Lesmes, U., Margier, M., Reboul, E., & Livney, Y. D. (2017). Re-assembled casein micelles improve in vitro bioavailability of vitamin D in a Caco-2 cell model. *Food Funct., 8*(6), 2133–2141. https://doi.org/10.1039/C7FO00323D

Dalgleish, D. G. (2011). On the structural models of bovine casein micelles—review and possible improvements. *Soft Matter, 7*(6), 2265–2272. https://doi.org/10.1039/C0SM00806K

De Kruif, C. G. (1999). Casein micelle interactions. *Int. Dairy J., 9*(3–6), 183–188. https://doi.org/10.1016/S0958-6946(99)00058-8

De Kruif, C. G., & Zhulina, E. B. (1996). κ-casein as a polyelectrolyte brush on the surface of casein micelles. *Colloids Surf. A Physicochem. Eng. Asp., 117*(1–2), 151–159. https://doi.org/10.1016/0927-7757(96)03696-5

Díez-Peña, E., Quijada-Garrido, I., & Barrales-Rienda, J. M. (2003). Analysis of the swelling dynamics of cross-linked p (N-iPAAm-c o-MAA) copolymers and their homopolymers under acidic medium. A kinetics interpretation of the overshooting effect. *Macromolecules, 36*(7), 2475–2483. https://doi.org/10.1021/ma021469c

Dumpler, J., Kieferle, I., Wohlschläger, H., & Kulozik, U. (2017). Milk ultrafiltrate analysis by ion chromatography and calcium activity for SMUF preparation for different scientific purposes and prediction of its supersaturation. *Int. Dairy J., 68*, 60–69. https://doi.org/10.1016/j.idairyj.2016.12.009

Eedara, B. B., Tucker, I. G., & Das, S. C. (2019). A STELLA simulation model for in vitro dissolution testing of respirable size particles. *Sci. Rep., 9*(1), 18522. https://doi.org/10.1038/s41598-019-55164-0

Farrell, H. M., Jr., Malin, E. L., Brown, E. M., & Qi, P. X. (2006). Casein micelle structure: What can be learned from milk synthesis and structural biology? *Curr. Opin. Colloid Interface Sci., 11*(2–3), 135–147. https://doi.org/10.1016/j.cocis.2005.11.005

Gebhardt, R., Khanna, S., Schulte, J., & Asaduzzaman, M. (2022). Effect of transglutaminase post-treatment on the stability and swelling behavior of casein micro-particles. *Int. J. Mol. Sci., 23*(19), 11837. https://doi.org/10.3390/ijms231911837

Gebhardt, R., Pechkova, E., Riekel, C., & Nicolini, C. (2010). In situ μGISAXS: II. Thaumatin crystal growth kinetic. *Biophys. J., 99*(4), 1262–1267. https://doi.org/10.1016/j.bpj.2010.03.068

Gebhardt, R., Pütz, T., & Schulte, J. (2023). Nearly reversible expansion and shrinkage of casein microparticles triggered by extreme pH changes. *Micromachines, 14*(3), 678. https://doi.org/10.3390/mi14030678

Heidebach, T., Först, P., & Kulozik, U. (2009a). Transglutaminase-induced caseinate gelation for the microencapsulation of probiotic cells. *Int. Dairy J., 19*(2), 77–84. https://doi.org/10.1016/j.idairyj.2008.08.003

Heidebach, T., Först, P., & Kulozik, U. (2009b). Microencapsulation of probiotic cells by means of rennet-gelation of milk proteins. *Food Hydrocoll., 23*(7), 1670–1677. https://doi.org/10.1016/j.foodhyd.2009.01.006

Holt, C., Carver, J. A., Ecroyd, H., & Thorn, D. C. (2013). Invited review: Caseins and the casein micelle: Their biological functions, structures, and behavior in foods. *J. Dairy Sci., 96*(10), 6127–6146. https://doi.org/10.3168/jds.2013-6831

Huaman, M. A. L., Vega-Chacón, J., Quispe, R. I. H., & Negrón, A. C. V. (2023). Synthesis and swelling behaviors of poly (2-hydroxyethyl methacrylate-co-itaconic acid) and poly (2-hydroxyethyl methacrylate-co-sodium itaconate) hydrogels as potential drug carriers. *Results in Chemistry, 5*, Article 100917. https://doi.org/10.1016/j.rechem.2023.100917

Huppertz, T., Smiddy, M. A., & de Kruif, C. G. (2007). Biocompatible micro-gel particles from cross-linked casein micelles. *Biomacromolecules, 8*(4), 1300–1305. https://doi.org/10.1021/bm061070m

de Kruif, C. K., Anema, S. G., Zhu, C., Havea, P., & Coker, C. (2015). Water holding capacity and swelling of casein hydrogels. *Food Hydrocoll., 44*, 372–379. https://doi.org/10.1016/j.foodhyd.2014.10.007

Lavoisier, A., Vilgis, T. A., & Aguilera, J. M. (2019). Effect of cysteine addition and heat treatment on the properties and microstructure of a calcium-induced whey protein cold-set gel. *Current Research in Food Science, 1*, 31–42. https://doi.org/10.1016/j.crfs.2019.10.001

Liu, Y., & Guo, R. (2007). Interaction between casein and sodium dodecyl sulfate. *J. Colloid Interface Sci., 315*(2), 685–692. https://doi.org/10.1016/j.jcis.2007.07.018

Lowe, E. K., Anema, S. G., Bienvenue, A., Boland, M. J., Creamer, L. K., & Jiménez-Flores, R. (2004). Heat-induced redistribution of disulfide bonds in milk proteins. 2. Disulfide bonding patterns between bovine β-lactoglobulin and κ-casein. *J. Agric. Food Chem., 52*(25), 7669–7680. https://doi.org/10.1021/jf0491254

Lucey, J. A. (2020). Milk protein gels. In *Milk proteins* (pp. 599–632). Academic Press. https://doi.org/10.1016/B978-0-12-405171-3.00017-9.

Mahomud, M. S., Haque, M. A., Akhter, N., & Asaduzzaman, M. (2021). Effect of milk pH at heating on protein complex formation and ultimate gel properties of free-fat yoghurt. *J. Food Sci. Technol., 58*, 1969–1978. https://doi.org/10.1007/s13197-020-04708-8

Menéndez-Aguirre, O., Kessler, A., Stuetz, W., Grune, T., Weiss, J., & Hinrichs, J. (2014). Increased loading of vitamin D2 in reassembled casein micelles with temperature-modulated high pressure treatment. *Food Res. Int., 64*, 74–80. https://doi.org/10.1016/j.foodres.2014.06.010

Mezzenga, R., & Fischer, P. (2013). The self-assembly, aggregation and phase transitions of food protein systems in one, two and three dimensions. *Rep. Prog. Phys., 76*(4), Article 046601. https://doi.org/10.1088/0034-4885/76/4/046601

Nguyen, N. H., Streicher, C., & Anema, S. G. (2018). The effect of thiol reagents on the denaturation of the whey protein in milk and whey protein concentrate solutions. *Int. Dairy J., 85*, 285–293. https://doi.org/10.1016/j.idairyj.2018.06.012

Ogieglo, W., de Grooth, J., Wormeester, H., Wessling, M., Nijmeijer, K., & Benes, N. E. (2013). Relaxation induced optical anisotropy during dynamic overshoot swelling of zwitterionic polymer films. *Thin Solid Films, 545*, 320–326. https://doi.org/10.1016/j.tsf.2013.07.077

Schott, H. (1992). Swelling kinetics of polymers. *Journal of Macromolecular Science, Part B: Physics, 31*(1), 1–9.

Schulte, J., Pütz, T., & Gebhardt, R. (2021). Statistical analysis of the swelling process of casein microparticles based on single particle measurements. *Food Hydrocolloids for Health, 1*, Article 100014. https://doi.org/10.1016/j.fhfh.2021.100014

Schulte, J., Pütz, T., & Gebhardt, R. (2022). Influence of pectin and drying conditions on the structure, stability and swelling behaviour of casein microparticles. *Int. Dairy J., 133*, Article 105422. https://doi.org/10.1016/j.idairyj.2022.105422

Schulte, J., Stöckermann, M., & Gebhardt, R. (2020). Influence of pH on the stability and structure of single casein microparticles. *Food Hydrocoll., 105*, Article 105741. https://doi.org/10.1016/j.foodhyd.2020.105741

Schulte, J., Stöckermann, M., Thill, S., & Gebhardt, R. (2020). Calcium effect on the swelling behaviour and stability of casein microparticles. *Int. Dairy J., 105*, Article 104692. https://doi.org/10.1016/j.idairyj.2020.104692

Shieh, L. Y., & Peppas, N. A. (1991). Solute and penetrant diffusion in swellable polymers. XI. The dynamic swelling behavior of hydrophilic copolymers containing multiethylene glycol dimethacrylates. *J. Appl. Polym. Sci., 42*(6), 1579–1587. https://doi.org/10.1002/app.1991.070420611

Song, F., Zhang, L. M., Yang, C., & Yan, L. (2009). Genipin-crosslinked casein hydrogels for controlled drug delivery. *Int. J. Pharm., 373*(1–2), 41–47. https://doi.org/10.1016/j.ijpharm.2009.02.005

Steinhauer, T., Kulozik, U., & Gebhardt, R. (2014). Structure of milk protein deposits formed by casein micelles and β-lactoglobulin during frontal microfiltration. *J. Membr. Sci., 468*, 126–132. https://doi.org/10.1016/j.memsci.2014.05.027

Takagi, H., Nakano, T., Aoki, T., & Tanimoto, M. (2022). Temperature dependence of the casein micelle structure in the range of 10–40° C: An in-situ SAXS study. *Food Chem., 393*, Article 133389. https://doi.org/10.1016/j.foodchem.2022.133389

Takagi, H., Nakano, T., Aoki, T., & Tanimoto, M. (2023). The structural changes of a bovine casein micelle during temperature change; in situ observation over a wide spatial scale from nano to micrometer. *Soft Matter, 19*(24), 4562–4570. https://doi.org/10.1039/D3SM00146F

Takagi, H., Nakano, T., Aoki, T., & Tanimoto, M. (2024). A SAXS and USAXS study of the influence of pH on the casein micelle structure. *Food Chem., 443*, Article 138606. https://doi.org/10.1016/j.foodchem.2024.138606

Tang, C. H. (2021). Strategies to utilize naturally occurring protein architectures as nanovehicles for hydrophobic nutraceuticals. *Food Hydrocoll., 112*, Article 106344. https://doi.org/10.1016/j.foodhyd.2020.106344

Thill, S., Schmidt, T., Jana, S., Wöll, D., & Gebhardt, R. (2022). Fine structure and swelling properties of fibers from regenerated rennet-treated casein micelles. *Macromolecular Materials and Engineering, 307*(10), 2200272.

Trejo, R., Dokland, T., Jurat-Fuentes, J., & Harte, F. (2011). Cryo-transmission electron tomography of native casein micelles from bovine milk. *J. Dairy Sci., 94*(12), 5770–5775. https://doi.org/10.3168/jds.2011-4368

Valencia, J., & Piérola, I. F. (2002). Swelling kinetics of poly (n-vinylimidazole-co-sodium styrenesulfonate) hydrogels. *J. Appl. Polym. Sci., 83*(1), 191–200. https://doi.org/10.1002/app.10059

Van Dijk, E., Hoogeveen, A., & Abeln, S. (2015). The hydrophobic temperature dependence of amino acids directly calculated from protein structures. *PLoS Comput. Biol., 11*(5), Article e1004277. https://doi.org/10.1371/journal.pcbi.1004277

Vasbinder, A. J., Alting, A. C., Visschers, R. W., & de Kruif, C. G. (2003). Texture of acid milk gels: Formation of disulfide cross-links during acidification. *Int. Dairy J., 13*(1), 29–38. https://doi.org/10.1016/S0958-6946(02)00141-3

Vasbinder, A. J., van de Velde, F., & de Kruif, C. G. (2004). Gelation of casein-whey protein mixtures. *J. Dairy Sci., 87*(5), 1167–1176. https://doi.org/10.3168/jds.S0022-0302(04)73265-8

Yin, Y., Ji, X., Dong, H., Ying, Y., & Zheng, H. (2008). Study of the swelling dynamics with overshooting effect of hydrogels based on sodium alginate-g-acrylic acid. *Carbohydr. Polym., 71*(4), 682–689. https://doi.org/10.1016/j.carbpol.2007.07.012

Zhuang, Y., Sterr, J., Kulozik, U., & Gebhardt, R. (2015). Application of confocal Raman microscopy to investigate casein micro-particles in blend casein/pectin films. *Int. J. Biol. Macromol., 74*, 44–48. https://doi.org/10.1016/j.ijbiomac.2014.11.017